

Structural and Electronic Effects of 1,3,4-Thiadiazole Units Incorporated into Polythiophene Chains

Hao Pang,[‡] Peter J. Skabara,^{*,‡} David J. Crouch,[†] Warren Duffy,[§] Martin Heeney,[§] Iain McCulloch,^{§,||} Simon J. Coles,[#] Peter N. Horton,[#] and Michael B. Hursthouse[#]

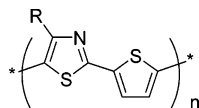
WestCHEM, Department of Pure and Applied Chemistry, University of Strathclyde, Glasgow G1 1XL, United Kingdom, School of Chemistry, University of Manchester, Manchester M13 9PL, United Kingdom, Merck Chemicals Chilworth Science Park, Southampton SO16 7QD, United Kingdom, and Department of Chemistry, University of Southampton, Highfield, Southampton SO17 1BJ, United Kingdom

Received June 4, 2007; Revised Manuscript Received July 6, 2007

ABSTRACT: A series of conjugated triaryl compounds have been synthesized, consisting of thiophene or selenophene peripheral units and a central 1,3,4-thiadiazole (TDA) heterocycle. X-ray crystallographic studies on four of the materials reveal that the molecules are planar in the solid state and feature an array of intramolecular (heteroatomic) and intermolecular (heteroatomic and π – π) noncovalent close contacts. Electrochemical oxidative polymerization affords insoluble polymers for **EDOT-TDA-EDOT** and **EDTT-TDA-EDTT**. The band gaps of the polymers have been deduced by cyclic voltammetry and electronic absorption spectroscopy and were found to be 1.8–1.9 eV. Both polymers show good stability toward n-doping and the EDTT analogue is more readily reduced than the EDOT-containing system. The enhanced stability toward n-doping, compared with the homopolymers PEDTT and PEDOT, is attributed to the presence of the electron deficient thiadiazole unit. The LUMO of poly(**EDTT-TDA-EDTT**) is 0.3 eV lower than that of poly(**EDOT-TDA-EDOT**), demonstrating that the substituent effect of the chalcogen atom is an important contributor to the electronic properties of the polymers.

Introduction

Conjugated oligomers and polymers have attracted much recent attention due to their interesting electronic and optical properties,¹ particularly in applications such as organic field effect transistors,^{2–4} solar cells,⁵ light emitting diodes,⁶ sensors⁷ and lasers.⁸ The incorporation of nitrogen-based heterocycles into the conjugated backbone facilitates n-doping, and these aromatic units can also influence the self-assembly of the macromolecule. For instance, it was reported that five-membered ring heteroaromatic π -conjugated polymers, such as alternating copolymers of 4-alkylthiazole and thiophene (PTz(R)Th), formed a unique π -stacked structure in the solid state assisted by a charge transfer (CT) electronic structure.⁹ The CT state is ascribed to the polymer's alternating electron-donating thiophene and electron-accepting thiazole units. Yamamoto et al. further investigated the material's packing ability in OFET devices.¹⁰ The copolymers demonstrated mobilities as high as $2.5 \times 10^{-3} \text{ cm}^2 \text{ V}^{-1} \text{ s}^{-1}$.



PTz(R)Th

In order to investigate the packing structure and properties of similar donor–acceptor π -conjugated copolymers, a series of new 1,3,4-thiadiazole-based π -conjugated polymers was targeted by choosing hexylthiophene, hexylselenophene, de-

cylthiophene, 3,4-ethylenedioxythiophene (EDOT), 3,4-ethylenedithiophene (EDTT), and 3,4-ethylenediselenothiophene (EDST) as the electron-donating units. The five-membered 1,3,4-thiadiazole, which incorporates two electron withdrawing imine (C=N) nitrogens, possesses a high electron affinity¹¹ and donor–acceptor π -conjugated systems consisting of these units are worth investigating as ambipolar/ambivalent materials. Although various charge transfer π -conjugated copolymers have been prepared and their optical and electronic properties investigated,^{12–17} π -conjugated polymers consisting of 1,3,4-thiadiazole electron-acceptors as core units have received less attention. Recently a copolymer of unsubstituted thiophene and 1,3,4-thiadiazole has been reported. Because of the lack of solubilizing side groups, the polymer was only soluble in trifluoroacetic acid into which the basic thiadiazole units would dissolve, nevertheless ambipolar field effect behavior with moderate charge carrier mobilities was reported.¹⁸ Oligo and polythiophenes containing 1,3,4-thiadiazole are considered to be of interest for several reasons. The electron-accepting thiadiazole architecture is expected to enhance stability toward oxygen (a prerequisite when considering device applications), as increasing the ionization potential of the material improves the stability of the material toward oxidative doping.¹⁹ The fused ring system is a planar rigid species containing no β -hydrogens thus reducing steric interactions and promoting efficient intermolecular π – π interactions.²⁰ The band gap energy of donor–acceptor oligomers is reduced compared to those of thiophene oligomers and the lower energy gap favors high carrier mobilities.²¹ Herein, we report the synthesis and characterization of a new family of triaryl systems containing central thiadiazole units and peripheral thiophenes or selenophenes. The corresponding polymers, prepared by electrochemical oxidation, have also been investigated and the effect of the thiadiazole unit on the structure and electronic properties of these materials is discussed.

* Corresponding author. E-mail: peter.skabara@strath.ac.uk.

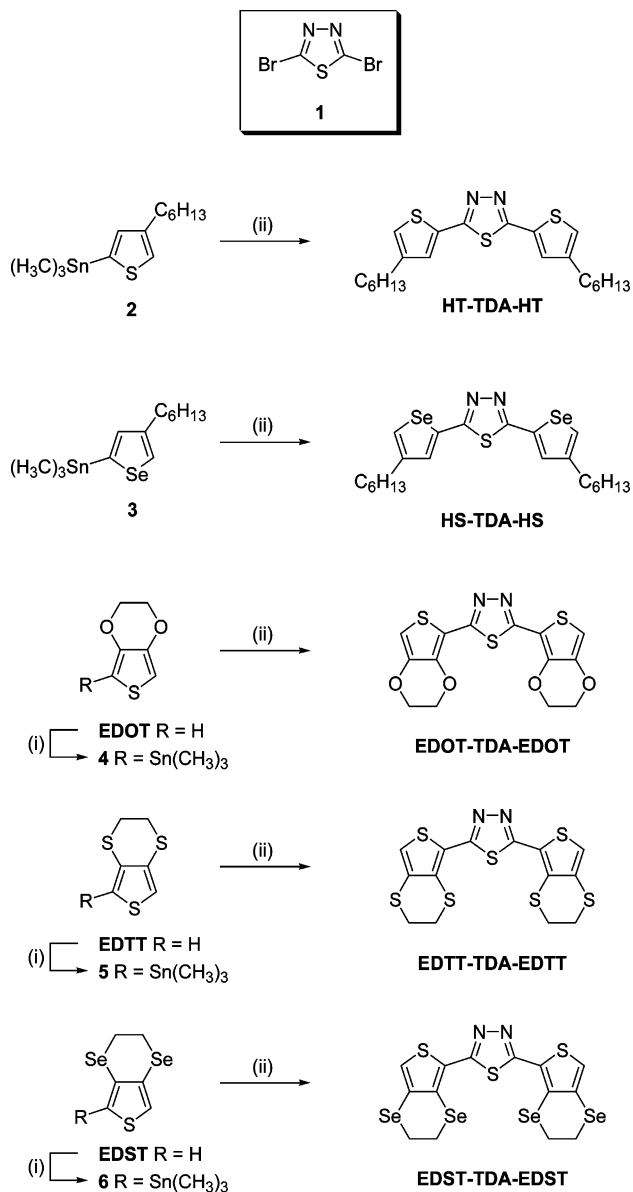
[‡] University of Strathclyde.

[†] University of Manchester.

[§] Merck Chemicals.

[#] University of Southampton.

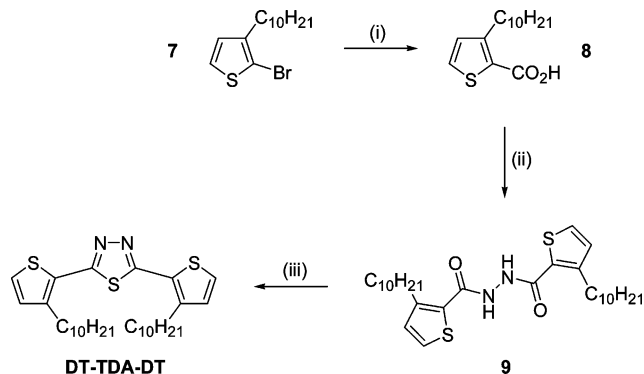
^{||} New address: Department of Chemistry, Imperial College London, Exhibition Road, London SW7 2AZ, United Kingdom.

Scheme 1^a

^a Reagents and conditions: (i) *n*-BuLi (LDA in the case of EDST), THF, -78°C , $(\text{CH}_3)_3\text{SnCl}$; (ii) 2,5-dibromo-1,3,4-thiadiazole (**1**), Pd(PPh₃)₄, μW , 300 W, DMF, 2 h.

Results and Discussion

Synthesis. The choice of thiophene derivatives was influenced by the following considerations: (i) incorporation of alkyl substituents at the 3 or 4 positions to form soluble polymers; (ii) incorporation of EDOT, EDTT and EDST to investigate the nature of intramolecular interactions (S–N; Se–N; S–S; S–O; S–Se) that could arise within the conjugated chains, along with different electronic effects of the chalcogen substituents. A 4-hexylselenophene derivative was prepared, to compare the properties of related thiophene/selenophene systems. 2,5-Dibromo-1,3,4-thiadiazole (**1**)⁹ was obtained from the reaction of 2-amino-5-bromo-1,3,4-thiadiazole by in situ diazotization with *tert*-butyl nitrite, followed by reaction with copper(II) bromide. Compound **1** was coupled to a series of thiophene derivatives under Stille conditions (Scheme 1). Procedures for the preparation of derivatives **2**,²² **3**,²³ EDOT,²⁴ EDTT^{25,26} and EDST²⁷ have been reported previously. Lithiation of EDOT, EDTT, and EDST was accomplished using *n*-BuLi or LDA at -78°C and the addition of trimethyltin chloride gave compounds **4–6** in

Scheme 2^a

^a Reagents and conditions: (i) Mg, THF, then CO_2 ; (ii) $(\text{COCl})_2$, then N_2H_4 , THF; (iii) Lawesson's reagent, xylene, 120°C .

86–95% yield (crude). Dichloromethane solutions of the stannylated compounds were washed with saturated ammonium chloride solution. After isolation of the organic phase, drying and removal of the solvent, derivatives **4–6** were used without further purification. The Stille coupling reactions were performed under microwave conditions to afford the corresponding triaryl derivatives in 16–78% yield. Notably, the stannylated EDChT (Ch = O, S, Se) series of compounds gave far higher yields (70–78%) for the coupling reactions than the alkyl derivatives **2** and **3** (16 and 18%). The synthesis of 2,5-bis(3-decylthiophen-2-yl)-1,3,4-thiadiazole (**DT-TDA-DT**) was afforded via an alternative strategy starting from 2-bromo-3-decylthiophene (**7**).²⁸ Synthesis of 3-alkylthiophene-2-carboxylic acid **8** was achieved via magnesium insertion using standard Grignard conditions followed by solid carbon dioxide addition and acid work up to yield **8** in 74% yield (Scheme 2). Conversion of the carboxylic acid **8** to the acid chloride was afforded using oxalyl chloride and this intermediate was treated in situ with hydrazine in THF to yield the hydrazide **9** in an overall yield of 58%. Ring closure of the symmetrical hydrazide was afforded in 76% yield using Lawesson's reagent in xylene at 120°C .

X-ray Crystallography. Understanding the morphology of conjugated polymers is important for the elucidation of physico-structural relationships. While the crystal structures of monomer units do not represent precisely the structure and self-assembly of the corresponding polymers, information can be generated relating to the nature of noncovalent intramolecular contacts and interchain π – π interactions that are common between small molecule and macromolecule analogues. Single crystals were obtained from compounds **HT-TDA-HT**, **HS-TDA-HS**, **DT-TDA-DT**, and **EDTT-TDA-EDTT**. The asymmetric units are shown in Figure 1. Compounds **HT-TDA-HT** and **HS-TDA-HS** are isostructural. The hexyl chains in these compounds lie in two different orientations, with one aligning in the plane of the conjugated unit and the other perpendicular to it. In the case of **DT-TDA-DT**, both alkyl chains are perpendicular to the aromatic units. In the majority of cases, the triaryl units are arranged in all-*anti* conformations; the exception to this is found in **DT-TDA-DT**, which exists as an *anti-syn* conformer. The decylthiophene containing derivative is disordered in the crystal and there are two discrete triaryl blocks within the asymmetric unit (only one of these is shown in Figure 1). All four compounds show a high degree of planarity between aromatic units with maximum torsion angles within the series in the range 168 – 177° (Table 1).

The molecules feature several noncovalent interactions between heteratoms, representing intramolecular and intermolecular close contacts. In all of the *anti* conformers, adjacent

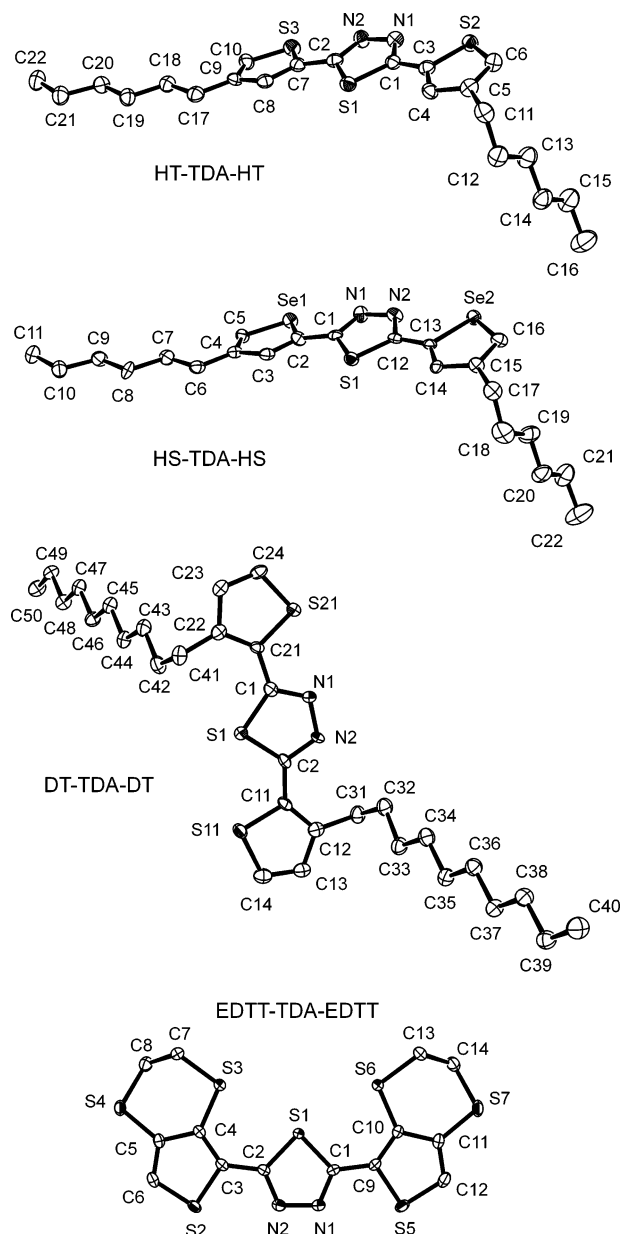


Figure 1. Asymmetric units of triaryl systems with Hs omitted for clarity.

thiadiazole-thiophene units (and thiadiazole-selenophene in the case of **HS-TDA-HS**) possess close contacts between N atoms and the chalcogen (2.91–3.05 Å for S \cdots N; 3.05–3.10 Å for Se \cdots N). For **EDTT-TDA-EDTT**, strong S \cdots S contacts also exist with interatomic distances of ca. 3.18 Å (Table 1).

The above are interactions that are likely to contribute to the planarization of the aromatic segments and this is an important feature for π – π stacking which facilitates charge transport through the bulk material. For conjugated materials bearing donor and acceptor aromatic units, we²⁹ and others^{30–33} have found that the electron rich and electron deficient ring systems form associations between chains that are electrostatic in nature. This is indeed the case for the compounds in this series, where the thiadiazole rings are sandwiched between thiophene units (see Figure 2 and Table 1 for π – π contacts). The association is illustrated in Figure 2a for **HT-TDA-HT** which also features interchain sulfur–sulfur contacts between aligned rings. Neighboring stacks are aligned such that the molecules are orthogonal to each other and feature interstack S \cdots N close contacts. In the selenium analogue, **HS-TDA-HS**, the π – π interactions and

chalcogen–chalcogen distances are slightly expanded due to the larger size of the selenium atom, but the contacts are shorter for the chalcogen–nitrogen associations due to the greater polarizability of the atom compared to sulfur. For **DT-TDA-DT**, the π – π interactions are strongest (in the range 3.4–3.9 Å) and adjacent stacks of molecules are interlinked through S \cdots N short contacts. The decyl chains are interdigitated in the structure, forming an insulating layer and ensuring that the range of intermolecular contacts are restricted within two dimensions. Inter-ring distances for **EDTT-TDA-EDTT** are 3.86 Å and adjacent stacks are held together through short S \cdots S contacts (S(2)–S(5) = 3.526(1) Å). There are no further supramolecular associations, so the structure can be considered to consist of close contacts in two dimensions only.

Absorption Spectroscopy and Electrochemistry of Monomers The six thiadiazole derivatives have been studied by cyclic voltammetry in dichloromethane solution using a silver wire reference electrode and tetrabutylammonium hexafluorophosphate as the supporting electrolyte (0.1 M). Under these conditions, **HT-TDA-HT** and **HS-TDA-HS** display one-electron irreversible oxidation peaks at +1.28 and +1.15 V, respectively, and one-electron irreversible reduction peaks at –2.26 and –2.22 V (Figure 3, Table 2). The HOMO and LUMO values of the compounds can be derived using ferrocene as an internal standard (Table 2). The HOMO value of **HT-TDA-HT** (–6.1 eV) is similar to that of **HS-TDA-HS** (–6.0 eV). Also, there are close LUMO values between **HT-TDA-HT** (–2.5 eV) and **HS-TDA-HS** (–2.6 eV). The difference in the HOMO–LUMO gaps for the two compounds (**HT-TDA-HT** = 3.6 eV; **HS-TDA-HS** = 3.4 eV) is the same as that derived from absorption spectroscopy (3.1 eV (λ_{max} = 353 nm) and 2.9 eV (λ_{max} = 370 nm), respectively; see Supporting Information). The smaller HOMO–LUMO gap for the selenium variant demonstrates the typical trend for direct sulfur/selenium analogues.²⁷ The redox data for **DT-TDA-DT** is different to its hexyl analogue and this could be explained by the fact that the alkyl chains are in different regiochemistries (see Supporting Information and Table 2). Although the HOMO–LUMO gaps are very similar, E_{lox} and E_{red} are lower for **DT-TDA-DT**, by 180 and 380 mV, respectively. The absorption maximum for **DT-TDA-DT** is only 8 nm lower than that for **HT-TDA-HT**, and the optically derived HOMO–LUMO gap is 3.1 eV.

The three compounds **EDOT-TDA-EDOT**, **EDTT-TDA-EDTT**, and **EDST-TDA-EDST** also undergo irreversible oxidation processes (Figure 4). **EDOT-TDA-EDOT** affords a small, sharp peak at +0.85 V followed by a larger peak at +1.25 V. **EDTT-TDA-EDTT** provides a more complex series of oxidation processes at +1.03, +1.17, and +1.57 V. Similarly, **EDST-TDA-EDST** gives peaks at +0.82, +1.10, +1.28, and +1.52 V. For reduction processes, **EDOT-TDA-EDOT** shows a small broad peak at –2.0 V and a strong sharper peak at –2.6 V, while the other two analogues afford peaks at –1.74 and –2.03 V (**EDTT-TDA-EDTT**) and –1.80 and –2.17 V (**EDST-TDA-EDST**). It is clear that the values for the HOMO–LUMO gaps in the EDChT (Ch = chalcogen) series are much lower than the hexylthiophene and hexylselenophene analogues (Table 2). Within the EDChT series, the only change in the chemical structure is the chalcogen atom and the HOMO–LUMO gap decreases in the trend O > S > Se. The absorption spectra for the EDChT series reveal fine structure (see Supporting Information section), indicative of rigid rod structures held in planar array through intramolecular noncovalent bonds.

Table 1. Structural Data Derived from Crystals of HT-TDA-HT, HS-TDA-HS, DT-TDA-DT, and EDTT-TDA-EDTT^b

	maximum torsion angle (deg)	N...S contact (intra, Å)	S...S contact (intra, Å)	X...Y contact (inter, Å)	π - π contact (inter, Å)
HT-TDA-HT	S(3)–C(7)–C(2)–S(1) 168.38(22)	N(2)–S(3) 3.046(4) N(1)–S(2) 3.005(4)	-	S(1)–S(2) 3.551(1) N(1)–S(2) 3.422(4) N(2)–S(2) 3.109(4)	3.76
HS-TDA-HS	Se(1)–C(2)–C(1)–S(1) 166.35(42)	N(1)–Se(1) 3.103(6) N(2)–Se(2) 3.053(6)	-	Se(2)–S(1) 3.617(2) N(1)–Se(2) 3.048(6) N(2)–Se(2) 3.369(6)	3.80
DT-TDA-DT	C(22)–C(21)–C(1)–N(1) 176.65(72)	N(1)–S(21) 2.916(2) N(102)–S(102) 2.982(25) ^a	-	N(102)–S(103) 3.090(16) N(101)–S(21) 3.356(16) N(1)–S(11) 3.146(12) N(2)–S(102) 3.313(10)	3.39 – 3.93
EDTT-TDA-EDTT	S(2)–C(3)–C(2)–S(1) 171.91(11)	N(1)–S(5) 2.911(2) N(2)–S(2) 2.913(2)	S(1)–S(6) 3.186(1) S(1)–S(3) 3.178(1)	S(2)–S(5) 3.526(1)	3.86

^a See Supporting Information section for the second triaryl moiety in the asymmetric unit of **DT-TDA-DT**. ^b Close contacts are those which are less than the sum of the van der Waals radii for the corresponding atoms: N, 1.55; S, 1.8; Se, 2.0 Å.³⁴

The corresponding absorption maxima for **EDOT-TDA-EDOT** (351, 365, and 383 nm), **EDTT-TDA-EDTT** (374, 392, and 412 nm), and **EDST-TDA-EDST** (382, 397, and 417 nm) follow the expected trend for the chalcogen substituent effect and the optical HOMO–LUMO gaps (3.1, 2.8, and 2.7 eV) match well with the values obtained by cyclic voltammetry.

Electrochemical Polymerization. The triaryl systems **EDOT-TDA-EDOT** and **EDTT-TDA-EDTT** were polymerized electrochemically by repetitive cycling over the anodic redox active range of the materials. The resulting polymers were dedoped for a period of 1 h in a region of electrochemical inactivity in a monomer-free acetonitrile solution and containing the same concentration of electrolyte. The voltammetric range for this procedure was determined by a 50–100 mV drop with respect to the emerging new oxidation process observed during electrochemical polymerization. The growth traces for the corresponding polymers are displayed in Figure 5. **EDOT-TDA-EDOT** and **EDTT-TDA-EDTT** polymerized readily, but **HT-TDA-HT**, **HS-TDA-HS**, and **EDST-TDA-EDST** showed resilience to polymerization, despite the use of a variety of solvents, working electrodes and scan rates. The relatively high oxidation potentials of **HT-TDA-HT** (+1.3 V) and **HS-TDA-HS** (+1.2 V) could be responsible for the failure of electrochemical polymerization of these two molecules. In the case of **EDST-TDA-EDST**, it should be noted that **EDST**²⁷ itself can be readily polymerized by electrochemical means, but there are several possible reasons why polymerization did not take place: (1) Relatively low oxidation potentials can lead to oligomeric (e.g., sexithiophene) products rather than long chain polymers.³⁵ The oxidation potential of **EDST-TDA-EDST** (+0.82 V) is significantly less than that of **EDTT-TDA-EDTT** (+1.03 V). (2) Low population of positive spin density of the resulting radical cation in the α -position of the peripheral thiophene.^{36–38} Substitution of oxygen at the β -positions for sulfur can lead to a statistical decrease for electrochemical coupling.^{37,39} The replacement of selenium for oxygen may have a greater impact in suppressing electrochemical polymerization. In the case of **DT-TDA-DT**, polymerization took place upon oxidation, but the film deposited on the anode gave poor quality voltammograms and showed signs of instability. The absorption spectrum

of a freshly made film clearly provides evidence for the formation of polymeric material, in which the π – π^* band of the monomer is shifted from 345 to 457 nm (see Supporting Information). Chemical polymerization was attempted using ferric chloride as the oxidant. Despite the functionalization of the polymer with two decyl chains per repeat unit, the resulting material proved to be highly insoluble. We attribute this to an extensive array of tight intermolecular contacts, based on those observed in the crystal structure of the monomer **DT-TDA-DT**.

The electrochemistry of the two polymers was investigated in acetonitrile and the corresponding data referenced to the ferrocene/ferrocenium redox couple. The cyclic voltammograms of poly(**EDOT-TDA-EDOT**) and poly(**EDTT-TDA-EDTT**) are shown in Figure 6 (see Table 3 for data). Both polymers give quasi-reversible oxidation and reduction processes. The oxidation potential of poly(**EDOT-TDA-EDOT**) is +0.14 V, which is 0.49 V lower than that of poly(**EDTT-TDA-EDTT**) ($E_{\text{ox}} = +0.63$ V), and is a direct result of the lower oxidation potential of the bis(EDOT) unit in the polymer structure, compared to bis(EDTT).⁴⁰ The reduction potential of poly(**EDOT-TDA-EDOT**) ($E_{\text{red}} = -2.10$ V) is 0.13 V more negative than that of the sulfur analogue ($E_{\text{red}} = -1.97$ V). The difference in E_{red} is attributed to the increased polarizability of the heavier chalcogen atom and this effect is observed nicely in the PEDChT series (Ch = O, S, Se) of polymers (Table 3). Both polymers show enhanced stability toward n-doping in relation to the related homopolymers PEDOT and PEDTT.

The electrochemical band gaps of poly(**EDOT-TDA-EDOT**) and poly(**EDTT-TDA-EDTT**) can be deduced from the difference between the onsets of reduction and oxidation processes, which represent the LUMO and HOMO bands, respectively. The two polymers possess similar band gap values of 1.8 and 1.9 eV. This is remarkably different from the values reported for the homopolymers PEDOT (1.3 eV) and PEDTT (2.2 eV).²⁷ Alternating donor–acceptor conjugated polymers can possess very low band gaps (i.e., < 1.4 eV).^{41–45} The thiadiazole unit in this work serves to lower the HOMOs and LUMOs for PEDOT and PEDTT and this would be expected for the

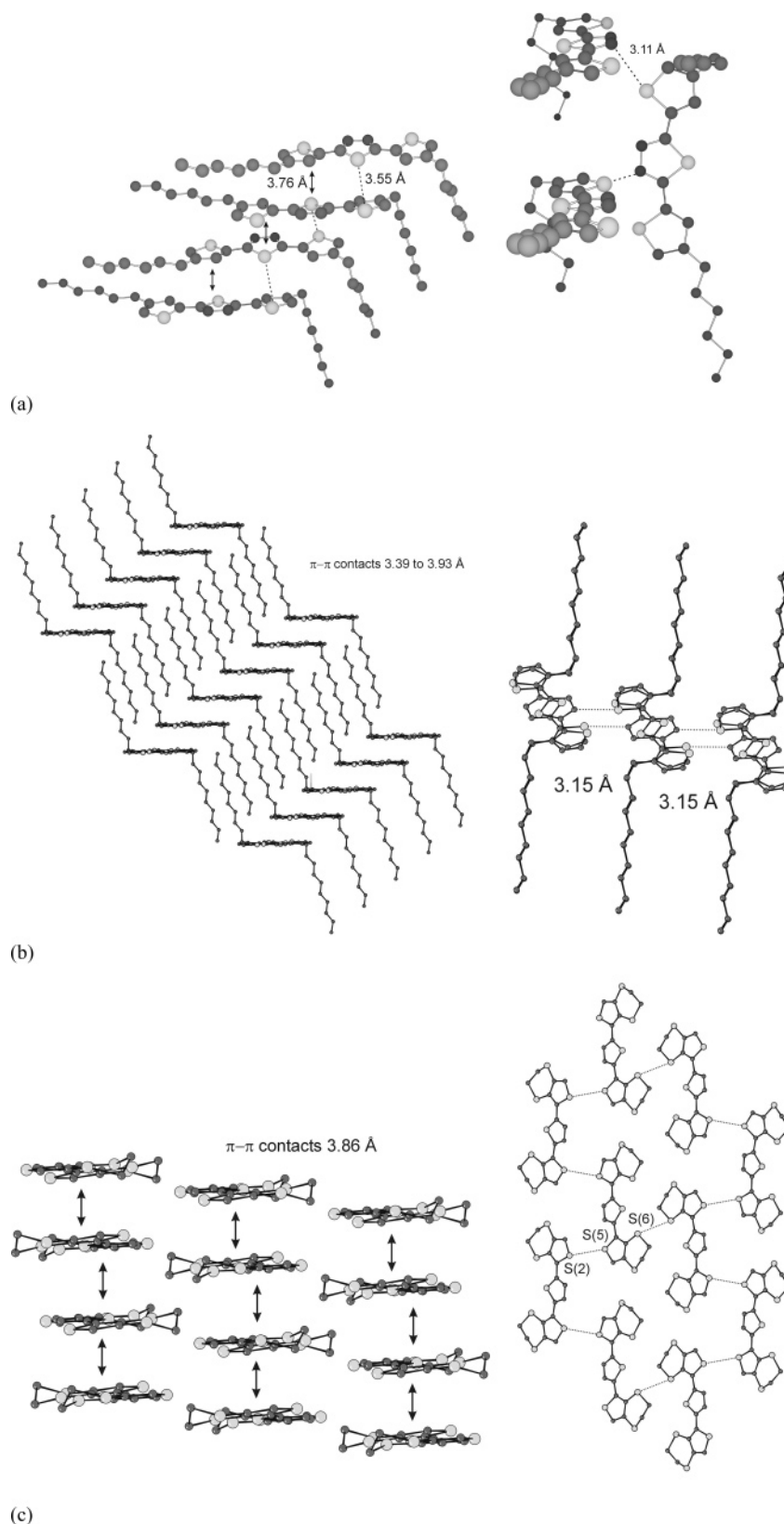


Figure 2. Packing of triaryl compounds for (a) **HT-TDA-HT**, (b) **DT-TDA-DT** (short contacts are shown for N(1)–S(11)), and (c) **EDTT-TDA-EDTT**, where the S...S distance is 3.526(1) Å.

incorporation of an acceptor unit into an electron rich backbone. The greatest changes are found between the HOMOs of PEDOT–poly(**EDOT-TDA-EDOT**) (0.7 eV) and the LUMOs of PEDTT–poly(**EDTT-TDA-EDTT**) (0.45 eV). However, the overall effect of incorporating the electron deficient thiadiazole unit is to narrow the band gap of the EDTT copolymer and

widen that of the EDOT analogue (with respect to the homopolymers PEDTT and PEDOT). Since an increase in conjugation leads to a smaller band gap, the result for poly(**EDTT-TDA-EDTT**) is reasonable to assume from the point of view that planarity could be retained within the repeat unit (see X-ray crystallographic section), whereas PEDTT is known

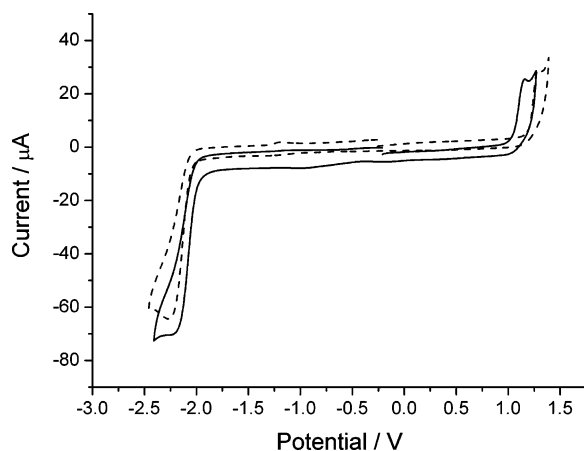


Figure 3. Cyclic voltammograms of compounds **HT-TDA-HT** (dashed line) and **HS-TDA-HS** (solid line). Experiments were conducted in CH_2Cl_2 solution, using a carbon working electrode, silver wire pseudo-reference, $(\text{TBA})\text{PF}_6$ as the supporting electrolyte (0.1 M), substrate concentration 10^{-3} M, and scan rate 100 mV/s. The data are referenced to the Fc/Fc^+ redox couple.

Table 2. Electrochemical Data for the Triaryl Compounds Derived by Cyclic Voltammetry, Where Experimental Conditions Are the Same as Those Given in Figures 3 and 4^a

monomer	E_{lox}/V	E_{red}/V	HOMO/ eV^a	LUMO/ eV^a	HOMO– LUMO gap/eV
HT-TDA-HT	+1.28	−2.26	−6.1	−2.5	3.6
HS-TDA-HS	+1.15	−2.22	−6.0	−2.6	3.4
DT-TDA-DT	+1.10	−2.64	−5.9	−2.2	3.7
EDOT-TDA-EDOT	+0.85	−2.0	−5.7	−2.8	2.9
EDTT-TDA-EDTT	+1.03	−1.74	−5.8	−3.0	2.8
EDST-TDA-EDST	+0.82	−1.80	−5.6	−3.0	2.6

^a HOMO and LUMO values are calculated from the first peak of the corresponding redox wave and referenced to ferrocene, which has a HOMO of -4.8 eV.

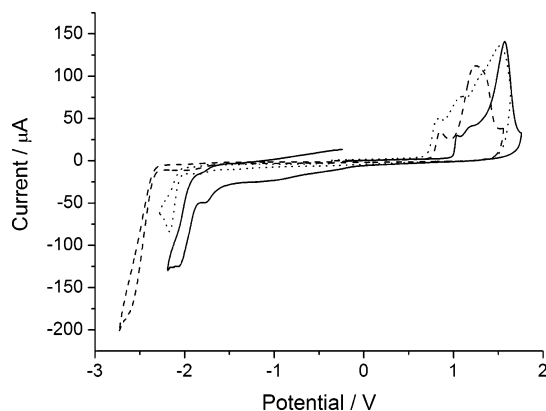


Figure 4. Cyclic voltammograms of **EDOT-TDA-EDOT** (dashed line), **EDTT-TDA-EDTT** (solid line), and **EDST-TDA-EDST** (dotted line) in CH_2Cl_2 solution, carbon working electrode, $(\text{TBA})\text{PF}_6$ as the supporting electrolyte (0.1 M), substrate concentration 10^{-3} M, scan rate 100 mV/s. The data are referenced to the Fc/Fc^+ redox couple.

to have a nonplanar structure throughout the chain.²⁴ In the case of poly(**EDOT-TDA-EDOT**), the LUMO is lowered by only 0.2 eV compared to PEDOT and it is the HOMO that is greatly affected. Assuming that oxidation takes place within the bis-(EDOT) units of poly(**EDOT-TDA-EDOT**), which are isolated by the thiadiazole units in the polymer chain, it follows that the oxidation potential of the polymer will be far higher than that of the infinite chain of EDOT units in PEDOT. This would explain the difference of 0.7 eV between the HOMOs of poly(**EDOT-TDA-EDOT**) and PEDOT.

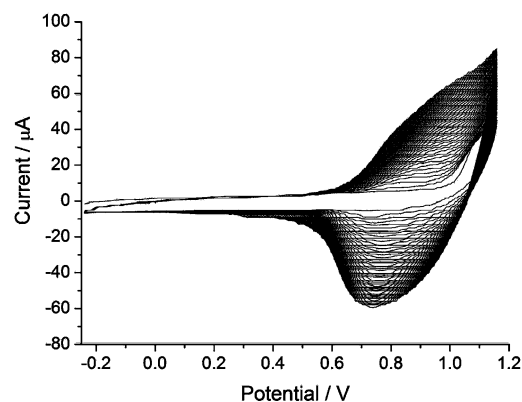
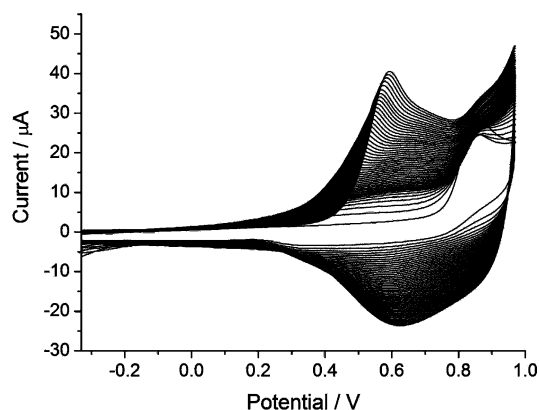


Figure 5. Growth of poly(**EDOT-TDA-EDOT**) (top) and poly(**EDTT-TDA-EDTT**) (bottom) by cyclic voltammetry in acetonitrile, using a carbon working electrode, Ag wire pseudo-reference electrode, $(\text{TBA})\text{PF}_6$ as the supporting electrolyte (0.1 M), substrate concentration 10^{-3} M, scan rate 300 mV/s. The data are referenced to the Fc/Fc^+ redox couple.

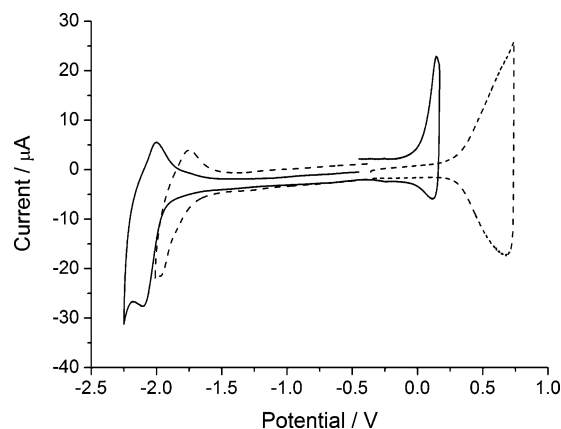
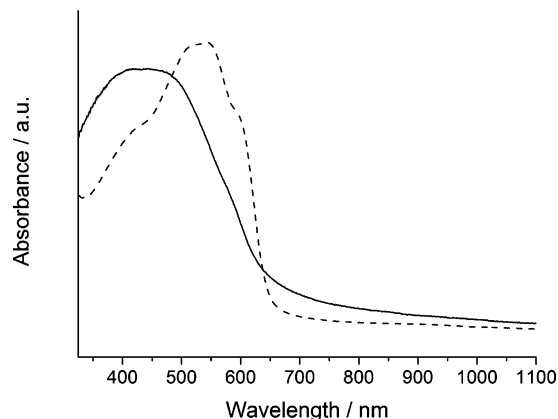


Figure 6. Cyclic voltammograms of poly(**EDOT-TDA-EDOT**) (continuous line) and poly(**EDTT-TDA-EDTT**) (dashed line) as films on a carbon working electrode. Experiments were conducted in monomer-free acetonitrile solution, under the same conditions as Figure 5. The data are referenced to the Fc/Fc^+ redox couple.

Further evidence that electrons are removed from a more localized site in poly(**EDOT-TDA-EDOT**) is obtained from absorption spectroelectrochemistry. The absorption spectrum of neutral poly(**EDOT-TDA-EDOT**) as a film gives a broad peak with a maximum centered at 433 nm and a shoulder at 572 nm (Figure 7, Table 3). Poly(**EDTT-TDA-EDTT**) gives a more resolved spectrum with peaks at 512, 546, and 593 nm, indicating a rigid conformation in the solid state. The optical band gaps of both polymers, calculated from the onset of the absorption bands, are in excellent agreement with the electro-

Table 3. Electrochemical and Absorption Spectroscopy Data for Thin Films of Poly(EDOT-TDA-EDOT), Poly(EDTT-TDA-EDTT), PEDOT, PEDTT, and PEDST

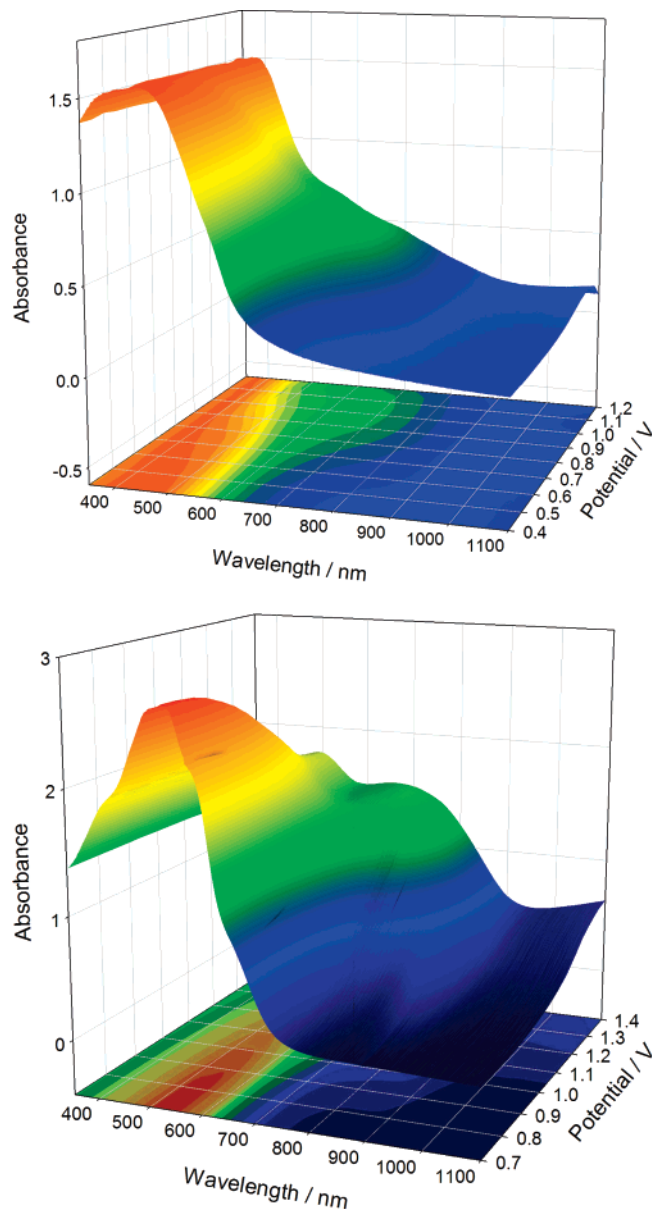
	HOMO (eV)	LUMO (eV)	E_g (echem, eV)	λ_{\max} (nm)	E_g (optical, eV)
poly(EDOT-TDA-EDOT)	-4.7	-2.9	1.8	433, 572	1.83
poly(EDTT-TDA-EDTT)	-5.1	-3.2	1.9	512, 546, 593	1.89
PEDOT ^a	-4.0	-2.7	1.3	578	1.6
PEDTT ^a	-4.9	-2.75	2.15	441	2.2
PEDST ^b	-4.8	-3.3	1.5	459	1.8

^a Data taken from ref 24. ^b Data obtained from ref 27.**Figure 7.** Electronic absorption spectra of poly(EDOT-TDA-EDOT) (solid line) and poly(EDTT-TDA-EDTT) (dashed line). Spectra were recorded on thin films on ITO glass.

chemical band gaps (Table 3). UV-vis spectroelectrochemical measurements were performed on films deposited on ITO glass over the oxidation range of both polymers. The spectroelectrochemical plot for poly(EDOT-TDA-EDOT) (Figure 8) is greatly different from that of PEDOT (see Supporting Information).²⁴ The optical transparency obtained upon p-doping PEDOT is lost in poly(EDOT-TDA-EDOT) and the generation of a new shallow peak at 692 nm for the latter and a hypsochromic shift of the $\pi-\pi^*$ band to 380 nm is representative of the formation of a localized positive polaron. The spectroelectrochemical plot for poly(EDTT-TDA-EDTT) is similar in nature to that of the oxygen analogue, but with a more intense fresh peak emerging at 741 nm and the $\pi-\pi^*$ band shifting to a lower wavelength of 506 nm. Again, the nature of the plot is vastly different to that of the PEDTT homopolymer, from which the bipolaron signature can be easily observed.²⁴

Conclusion

A series of conjugated molecules containing the electron deficient 1,3,4-thiadiazole unit have been synthesized and characterized by X-ray crystallography, cyclic voltammetry and absorption spectroscopy. The compounds are highly planar and assemble into tight packing structures through a variety of noncovalent heteroatomic and $\pi-\pi$ intermolecular contacts. These interactions are extremely important for charge transport properties, but the issue of insolubility needs to be addressed if polymeric materials are to be used in device applications. The cyclic systems **EDChT-TDA-EDChT** (where Ch = O, S, Se) are oxidized and reduced more easily than the alkyl analogues, demonstrating significant electronic substituent effects from the chalcogen atoms. Polymers have been obtained from the electrochemical oxidation of **EDOT-TDA-EDOT** and **EDTT-TDA-EDTT**. The electronic properties of the donor-acceptor copolymers are very different from their corresponding homopolymers PEDOT and PEDTT and, as expected, the thiadiazole containing polymers are more readily reduced and show

**Figure 8.** Absorption spectroelectrochemical plots for poly(EDOT-TDA-EDOT) (above) and poly(EDTT-TDA-EDTT) (below).

improved stability in their n-doped state. Cyclic voltammetry and electronic absorption spectroelectrochemistry show that in the p-doped state the polarons are localized within the bis-EDOT and bis-EDTT units for both polymers.

Experimental Section

Crystal Structure Analyses. Suitable crystals were selected and data for **HT-TDA-HT**, **HS-TDA-HS**, **EDTT-TDA-EDTT**, and **DT-TDA-DT** were measured on a Bruker Nonius KappaCCD Area detector equipped with a Bruker Nonius FR591 rotating anode ($\lambda_{\text{Mo-K}\alpha} = 0.71073 \text{ \AA}$) at 120 K driven by COLLECT,⁴⁶ processed by DENZO⁴⁷ software and corrected for absorption by using SADABS.⁴⁸ The structures were determined in SHELXS-97 and

refined using SHELXL-97.⁴⁹ All non-hydrogen atoms were refined anisotropically with hydrogen atoms included in idealized positions with thermal parameters riding on those of the parent atom. Crystal data and refinement results for all samples are collated in the Supporting Information.

General Data. All starting materials and reagents were purchased from Sigma-Aldrich or Lancaster Synthesis and used as received with the exception of 2-decyl-thiophene, which was purchased from Honeywell Specialty Chemicals GmbH and used as received. Bromination of 2-decylthiophene was carried out as reported in the literature.²⁸ Microwave reactions were performed with a Biotage Initiator EXP-EU.

Melting points were taken using a Stuart Scientific SMP1 melting point apparatus and are uncorrected. ¹H and ¹³C NMR spectra were recorded on a Bruker DPX instrument at 400 and 100 MHz; chemical shifts are given in parts per million. IR spectra for the characterization of the compounds were recorded on a Perkin-Elmer FTIR spectrometer. Mass spectra were recorded on a ThermoFinnigan LCQ DUO mass spectrometer and a Polaris Q TRACE GC 2000. Elemental analyses were obtained on a Perkin-Elmer 2400 elemental analyzer. Absorption spectra were measured on a Unicam UV 300 spectrophotometer. Electrochemical measurements were performed on a CH Instruments 660A electrochemical workstation with IR compensation using anhydrous dichloromethane or acetonitrile as the solvent, silver wire as the pseudo reference electrode, and platinum wire and glassy carbon as the counter and working electrodes, respectively. Electrochemical data were referenced to the ferrocene/ferrocenium redox couple using the metallocene as an internal standard. All solutions were degassed (Ar) and contained monomer substrates in concentrations of ca. 1×10^{-3} M, together with *n*-Bu₄NPF₆ (0.1 M) as the supporting electrolyte. Spectroelectrochemical experiments were conducted on ITO glass. The reactions were monitored by thin layer chromatography (TLC) using Merck silica gel 60 F₂₅₄ TLC plates and gas chromatography using an Agilent 6890 gas chromatograph equipped with an Agilent 5973 mass spectral detector.

Electrochemical Polymerization. Electrochemical polymerizations were carried out under potentiostatic conditions over the oxidation potentials of the **EDOT-TDA-EDOT** and **EDTT-TDA-EDTT** monomers at ambient temperature in a three-electrode single-compartment cell containing 0.1 M (TBA)PF₆ in 10 mL of dichloromethane. The working electrode was a carbon disk electrode and the counter electrode was platinum wire. A silver wire was used as the reference electrode. The solution was degassed by bubbling argon for 5 min prior to use and maintained under an argon blanket throughout each experiment. Thin films for electrochemical characterization were deposited on the small area carbon disk electrode at the oxidation potentials of **EDOT-TDA-EDOT** and **EDTT-TDA-EDTT** for 10 min. The polymer covered working electrode was then removed, washed with fresh acetonitrile, dried, and then transferred to another cell containing monomer-free (TBA)PF₆ acetonitrile solution for cyclic voltammetric analysis. Neutral (dedoped) polymer was obtained by electrochemically reducing the doped films at -0.2 to $+0.2$ V. Polymers were grown on ITO glass for spectroelectrochemical experiments.

General Procedure for the Formation of Compounds 4–6. To a solution of EDOT, EDTT, or EDST (10 mmol) in anhydrous THF (30 mL) was added dropwise *n*-butyllithium (2.5 M) (11 mmol) or LDA (1.5 M) (11 mmol, for EDST) at -78 °C. The mixture was stirred at this temperature for 1 h. Trimethyltin chloride (1.0 M in hexane) (11 mmol) was added dropwise and the resulting mixture was stirred at -78 °C for 1 h before allowing to warm to room temperature overnight. The solvent was removed by rotary evaporation and the resulting mixture was partitioned between CH₂-Cl₂ and saturated ammonium chloride solution. The organic layer was separated, washed with water, dried with MgSO₄ and filtered. The solvent was removed by rotary evaporation to afford a yellow oil in each case. These compounds were used without further purification.

2-(Trimethylstannyl)-3,4-ethylenedioxythiophene (4). Yield: 90%. ¹H NMR (CDCl₃): 0.23 (9H, s, CH₃), 3.98 (4H, s, CH₂),

6.14 (1H, s, CH). MS: *m/z* (EI) 305 (M⁺, 20%), 290 (100%).

2-(Trimethylstannyl)-3,4-ethylenedithiophene (5). Yield: 95%. ¹H NMR (CDCl₃): 0.45 (9H, s, CH₃), 3.26 (4H, s, CH₂), 7.25 (1H, s, CH); MS: *m/z* (EI) 338 (M⁺, 45%), 323 (100%).

2-(Trimethylstannyl)-3,4-ethylenediselenothiophene (6). Yield: 86%. ¹H NMR (CDCl₃): 0.35 (9H, s, CH₃), 3.22 (4H, s, CH₂), 7.43 (1H, s, CH); MS: *m/z* (EI) 432 (M⁺, 20%), 417 (30%).

General Procedure for the Formation of Triaryl Derivatives. The target compounds were prepared via microwave-assisted Stille coupling methodology in 2 h using microwave irradiation at 300 W. 2,5-Dibromo-1,3,4-thiadiazole (**1**) (0.3 mmol), the corresponding trimethylstannyl compound (0.65 mmol, 2.2 equiv), and tetrakis-(triphenylphosphine)palladium (0.1 equiv) were added to the microwave reaction tube, together with anhydrous DMF (3 mL). The reaction time was set to 2 h and the temperature to 160 °C. The resulting mixture was washed with chloroform, 2 M HCl, and then water. The solvent was removed by rotary evaporation, and the crude compounds were purified by flash chromatography. Subsequent recrystallization afforded the monomers in analytically pure form.

2,5-Bis(4-hexylthien-2-yl)-1,3,4-thiadiazole (HT-TDA-HT). Yield: 18%. ¹H NMR (CDCl₃): 0.89–0.93 (6H, t, *J* = 16.9 Hz), 1.31–1.32 (12H, m), 1.59–1.67 (4H, m), 2.59–2.63 (4H, t, *J* = 18.5 Hz), 7.06 (2H, s), 7.37 (2H, s). ¹³C NMR (CDCl₃): 14.2, 22.7, 29.1, 29.9, 30.5, 31.8, 124.3, 130.7, 132.0, 144.5, 161.2; MS: *m/z* (EI) 419 (M⁺, 100%); Anal. Calcd for C₂₂H₃₀N₂S₃: C, 63.11; H, 7.22; N, 6.69; S, 22.97. Found: C, 63.10; H, 7.48; N, 6.61; S, 23.02. IR: 2954, 1553, 1468, 1401, 1088, 868, 767, 581. Mp: 52–53 °C.

2,5-Bis(4-hexylselen-2-yl)-1,3,4-thiadiazole (HS-TDA-HS). Yield: 16%. ¹H NMR (CDCl₃): 0.89–0.92 (6H, t, *J* = 16.7 Hz), 1.27–1.39 (12H, m), 1.59–1.67 (4H, m), 2.57–2.61 (4H, t, *J* = 18.5 Hz), 7.55 (2H, s), 7.67 (2H, s). ¹³C NMR (CDCl₃): 14.3, 22.8, 29.1, 30.4, 31.8, 32.2, 128.8, 133.7, 136.2, 146.2, 163.0. MS: *m/z* AP⁺ 514 ([M + H]⁺, 100%). Anal. Calcd for C₂₂H₃₀N₂SSe₂: C, 51.56; H, 5.90; N, 5.47. Found: C, 51.84; H, 5.93; N, 5.71. IR: 2951, 1556, 1462, 1401, 1119, 1094, 834, 782, 568. Mp: 60–61 °C.

2,5-Bis(3,4-ethylenedioxythiophen-2-yl)-1,3,4-thiadiazole (EDOT-TDA-EDOT). Yield: 72%. ¹H NMR (CDCl₃): 3.22–3.24 (4H, t, *J* = 9.9 Hz), 4.36–4.38 (4H, t, *J* = 9.9 Hz), 6.44 (2H, s). MS: MALDI 366 (M⁺, 100%). Anal. Calcd for C₁₄H₁₀N₂O₄S₃: C, 45.89; H, 2.75; N, 7.64. Found: C, 45.85; H, 2.73; N, 7.52%. IR: 3090, 2963, 2923, 1509, 1423, 1278, 1185, 903, 752, 693, 639, 562. Mp: 302–304 °C.

2,5-Bis(3,4-ethylenedithiophen-2-yl)-1,3,4-thiadiazole (EDTT-TDA-EDTT). Yield: 78%. ¹H NMR (CDCl₃): 3.17–3.22 (4H, t, *J* = 12.8 Hz), 3.33–3.36 (4H, t, *J* = 12.8 Hz), 7.07 (2H, s). MS: *m/z* AP⁺ 431 ([M + H]⁺, 100%). Anal. Calcd for C₁₄H₁₀N₂S₇: C, 39.04; H, 2.34; N, 6.50; S, 52.11. Found: C, 38.92; H, 2.35; N, 6.39; S, 51.63. IR: 3086, 2962, 2921, 1501, 1416, 1284, 1141, 874, 758, 688, 652, 564. Mp: 250–251 °C.

2,5-Bis(3,4-ethylenediselenothiophen-2-yl)-1,3,4-thiadiazole (EDST-TDA-EDST). Yield: 70%. ¹H NMR (CDCl₃): 3.30–3.31 (4H, t, *J* = 13.9 Hz), 3.38–3.40 (4H, t, *J* = 13.9 Hz), 7.34 (2H, s). MS: MALDI 618 (M⁺, 50%). Anal. Calcd for C₁₄H₁₀N₂S₃Se₄: C, 27.20; H, 1.63; N, 4.53. Found: C, 27.05; H, 1.61; N, 4.45. IR: 3084, 2964, 2919, 1495, 1417, 1267, 1124, 880, 733, 646, 583. Mp: 238–240 °C.

3-Decylthiophene-2-carboxylic Acid (8). A mixture of magnesium (1.39 g, 0.049 mol) and 2-bromo-3-decylthiophene (**7**) (15.00 g, 0.057 mol) in THF (50 mL) was heated at 60 °C for 1 h. A small crystal of iodine was used to initiate the reaction. The reaction mixture was added in one portion to crushed cardice (150 g). Diethyl ether (200 mL) was added. The mixture was allowed to warm to room temperature. 10% aqueous HCl solution (200 mL) was carefully added to the mixture portion-wise with stirring. The layers were separated. The organic layer was washed with brine (2 × 150 mL) then dried (MgSO₄). After filtration the solvent was removed under reduced pressure to yield a yellow oil. The oil was dissolved in an acetonitrile/THF mixture and cooled slowly. After

a cold filtration the product was dried in vacuo. Yield: 9.85 g, 74%. ^1H NMR (CDCl_3 , 300 MHz): 0.88 (3H, t), 1.14–1.41 (14H, m), 1.63 (2H, quint), 3.02 (2H, t), 6.99 (1H, d, $J = 5.1$ Hz), 7.49 (1H, d, $J = 5.1$ Hz). ^{13}C NMR (CDCl_3 , 75 MHz): 14.14, 22.70, 29.35, 29.47, 29.51, 29.59, 29.63, 29.73, 30.45, 31.92, 125.79, 131.01, 131.01, 153.22, 167.94.

3-Decylthiophene-2-carboxylic Acid *N'*-(3-decyl-thiophene-2-carbonyl)hydrazide (9). 3-Decylthiophene-2-carboxylic acid (**8**) (9.00 g, 0.035 mol) was added to oxalyl chloride (50 mL) portionwise. The mixture was stirred at room temperature until all the acid had dissolved. The excess oxalyl chloride was removed by distillation to yield an orange oil. Yield: 9.00 g, 91.8%. A solution of hydrazine in THF (15.1 mL, 1.0 M solution in THF) was added via syringe to a mixture of the acid chloride (9.00 g, 0.03 mol) and triethylamine (5 mL) in THF (30 mL) at -5°C . The reaction mixture was allowed to warm to room temperature and stirred for a further 3 h. The reaction mixture was passed through a silica filter eluting with dichloromethane. Fractions containing the product were combined and recrystallized from dichloromethane. A second recrystallization from acetonitrile yielded pure material. Yield: 4.60 g, 58%. ^1H NMR (CDCl_3 , 300 MHz): 0.87 (6H, t), 1.17–1.42 (28H, m), 1.66 (4H, quint), 2.97 (4H, t), 6.99 (2H, d, $J = 4.9$ Hz), 7.37 (2H, d, $J = 5.1$ Hz), 8.54 (2H, s). ^{13}C NMR (CDCl_3 , 75 MHz): 14.16, 22.72, 29.37, 29.52, 29.57, 29.63, 29.64, 29.74, 30.63, 31.93, 126.58, 127.97, 130.93, 149.09, 160.17.

2,5-Bis(3-decylthiophen-2-yl)-1,3,4-thiadiazole (DT-TDA-DT). A mixture of 3-decylthiophene-2-carboxylic acid *N'*-(3-decylthiophene-2-carbonyl)hydrazide (**9**) (4.00 g, 0.075 mol) and Lawesson's reagent (3.64 g, 0.090 mol) in xylene (40 mL) was heated at 120°C overnight. The reaction mixture was filtered through neutral alumina, washing through with CH_2Cl_2 . Concentration of the filtrate gave 4.52 g of crude yellow oil. The crude material was dissolved in CH_2Cl_2 and purified by column chromatography on silica gel using CH_2Cl_2 as the eluent. The desired fractions were collected and concentrated to yield 3.02 g of a yellow oil. The oil crystallized on standing at room temperature. The product was recrystallized from a mixture of acetonitrile/THF to yield the pure product. Yield: 3.02 g, 76%. ^1H NMR (CDCl_3 , 300 MHz): 0.87 (6H, t), 1.18–1.48 (28H, m), 1.70 (4H, quint), 2.95 (4H, t), 7.01 (2H, d, $J = 5.3$ Hz), 7.39 (2H, d, $J = 5.1$ Hz). ^{13}C NMR (CDCl_3 , 75 MHz): 14.15, 22.71, 29.37, 29.52, 29.63, 29.64, 30.19, 31.93, 126.58, 128.08, 130.55, 144.63, 160.17. MS: EI 530 (M^+ , 10%). Anal. Calcd for $\text{C}_{30}\text{H}_{46}\text{N}_2\text{S}_3$: C, 67.9; H, 8.7; N, 5.3. Found: C, 67.7; H, 8.6; N, 5.4%. MPt $37-38^\circ\text{C}$.

Supporting Information Available: A figure showing the second molecule of **DT-TDA-DT** in the asymmetric unit, cif files, and tables giving the crystal data and refinement results for all samples, and figures showing the absorption spectra of compounds **HT-TDA-HT**, **DT-TDA-DT** and **HS-TDA-HS**, cyclic voltammograms of compounds **HT-TDA-HT**, **DT-TDA-DT** and **HS-TDA-HS**, absorption spectra of compounds **EDOT-TDA-EDOT**, **EDTT-TDA-EDTT** and **EDST-TDA-EDST**, absorption spectra of **DT-TDA-DT** in dichloromethane and poly(**DT-TDA-DT**) on ITO glass, and absorption spectroelectrochemical plot of PEDOT. This material is available free of charge via the Internet at <http://pubs.acs.org>.

References and Notes

- Shirota, Y.; Kageyama, H. *Chem. Rev.* **2007**, *107*, 953–1010.
- Facchetti, A. *Mater. Today* **2007**, *10*, 28–37.
- Murphy, A. R.; Frechet, J. M. J. *Chem. Rev.* **2007**, *107*, 1066–1096.
- Zaumseil, J.; Sirringhaus, H. *Chem. Rev.* **2007**, *107*, 1296–1323.
- Gunes, S.; Neugebauer, H.; Sariciftci, N. S. *Chem. Rev.* **2007**, *107*, 1324–1338.
- Müllen, K.; Scherf, U. *Organic Light-Emitting Devices, Synthesis, Properties and Applications*; Wiley-VCH: Weinheim, Germany, 2006.
- Thomas, S. W.; Joly, G. D.; Swager, T. M. *Chem. Rev.* **2007**, *107*, 1339–1386.
- Samuel, I. D. W.; Turnbull, G. A. *Chem. Rev.* **2007**, *107*, 1272–1295.
- Yasuda, T.; Imase, T.; Sasaki, S.; Yamamoto, T. *Macromolecules* **2005**, *38*, 1500–1503.
- Yamamoto, T.; Kokubo, H.; Kobashi, M.; Sakai, Y. *Chem. Mater.* **2004**, *16*, 4616–4618.
- Brocks, G.; Tol, A. *Synth. Met.* **1999**, *101*, 516–517.
- Zhu, Y.; Champion, R. D.; Jenekhe, S. A. *Macromolecules* **2006**, *39*, 8712–8719.
- Jenekhe, S. A.; Lu, L. D.; Alam, M. M. *Macromolecules* **2001**, *34*, 7315–7324.
- Yamamoto, T.; Kimura, T.; Shiraishi, K. *Macromolecules* **1999**, *32*, 8886–8896.
- Lee, B. L.; Yamamoto, T. *Macromolecules* **1999**, *32*, 1375–1382.
- Yao, Y. X.; Zhang, Q. T.; Tour, J. M. *Macromolecules* **1998**, *31*, 8600–8606.
- Zhang, Q. T.; Tour, J. M. *J. Am. Chem. Soc.* **1998**, *120*, 5355–5362.
- Yamamoto, T.; Yasuda, T.; Sakai, Y.; Aramaki, S.; Ramaw, A. *Macromol. Rapid Commun.* **2005**, *26*, 1214–1217.
- Li, W. J.; Katz, H. E.; Lovinger, A. J.; Laquindanum, J. G. *Chem. Mater.* **1999**, *11*, 458–465.
- Kwon, K. Y.; Lin, X.; Pawin, G.; Wong, K.; Bartels, L. *Langmuir* **2006**, *22*, 857–859.
- Ando, S.; Nishida, J.; Inoue, Y.; Tokito, S.; Yamashita, Y. *J. Mater. Chem.* **2004**, *14*, 1787–1790.
- Barbarella, G.; Bongini, A.; Zambianchi, M. *Macromolecules* **1994**, *27*, 3039–3045.
- Crouch, D. J.; Skabara, P. J.; Heeney, M.; McCulloch, I.; Sparrowe, D.; Coles, S. J.; Hursthouse, M. B. Manuscript in preparation.
- Spencer, H. J.; Skabara, P. J.; Giles, M.; McCulloch, L.; Coles, S. J.; Hursthouse, M. B. *J. Mater. Chem.* **2005**, *15*, 4783–4792.
- Wang, C. G.; Schindler, J. L.; Kannewurf, C. R.; Kanatzidis, M. G. *Chem. Mater.* **1995**, *7*, 58–68.
- Goldoni, F.; Langeveld-Voss, B. M. W.; Meijer, E. W. *Synth. Commun.* **1998**, *28*, 2237–2244.
- Pang, H.; Skabara, P. J.; Gordeyev, S.; McDouall, J. J. W.; Coles, S. J.; Hursthouse, M. B. *Chem. Mater.* **2007**, *19*, 301–307.
- Bauerle, P.; Pfau, F.; Schlupp, H.; Wurthner, F.; Gaudl, K. U.; Caro, M. B.; Fischer, P. *J. Chem. Soc., Perkin Trans.* **1993**, *5*, 489–494.
- Crouch, D. J.; Skabara, P. J.; Lohr, J. E.; McDouall, J. J. W.; Heeney, M.; McCulloch, I.; Sparrowe, D.; Shkunov, M.; Coles, S. J.; Horton, P. N.; Hursthouse, M. B. *Chem. Mater.* **2005**, *17*, 6567–6578.
- Reichenbacher, K.; Suss, H. I.; Hulliger, J. *Chem. Soc. Rev.* **2005**, *34*, 22–30.
- Dai, C. Y.; Nguyen, P.; Marder, T. B.; Scott, A. J.; Clegg, W.; Viney, C. *Chem. Commun.* **1999**, 2493–2494.
- Coates, G. W.; Dunn, A. R.; Henling, L. M.; Ziller, J. W.; Lobkovsky, E. B.; Grubbs, R. H. *J. Am. Chem. Soc.* **1998**, *120*, 3641–3649.
- Nae, D. G. *Acta Crystallogr. Sect. B, Struct. Sci.* **1979**, *35*, 2765–2768.
- Bondi, A. *J. Phys. Chem.* **1964**, *68*, 441.
- Henderson, P. T.; Collard, D. M. *Chem. Mater.* **1995**, *7*, 1879–1889.
- Tsai, E. W.; Basak, S.; Ruiz, J. P.; Reynolds, J. R.; Rajeshwar, K. *J. Electrochem. Soc.* **1989**, *136*, 3683–3689.
- Ruiz, J. P.; Nayak, K.; Marynick, D. S.; Reynolds, J. R. *Macromolecules* **1989**, *22*, 1231–1238.
- Ruiz, J. P.; Gieselman, M. B.; Nayak, K.; Marynick, D. S.; Reynolds, J. R. *Synth. Met.* **1989**, *28*, C481–C486.
- Roncali, J. *Chem. Rev.* **1992**, *92*, 711–738.
- Turbie, M.; Frere, P.; Allain, M.; Gallego-Planas, N.; Roncali, J. *Macromolecules* **2005**, *38*, 6806–6812.
- Akoudad, S.; Roncali, J. *Chem. Commun.* **1998**, 2081–2082.
- Kitamura, C.; Tanaka, S.; Yamashita, Y. *Chem. Mater.* **1996**, *8*, 570–578.
- Ho, H. A.; Brisset, H.; Frere, P.; Roncali, J. *J. Chem. Soc., Chem. Commun.* **1995**, 2309–2310.
- Havinga, E. E.; Tenhoeve, W.; Wynberg, H. *Synth. Met.* **1993**, *55*, 299–306.
- Ferraris, J. P.; Lambert, T. L. *J. Chem. Soc., Chem. Commun.* **1991**, 1268–1270.
- COLLECT: Data collection software; Hooft, R.; Nonius, B. V. 1998.
- Otwinowski, Z.; Minor, W. *Methods Enzymol.* **1997**, *276*, 307–326.
- Sheldrick, G. M. *SADABS, version 2.10*; Bruker AXS Inc.: Madison, WI, 2003.
- Sheldrick, G. M. *SHELX-97-Programs for crystal structure determination (SHELXS) and refinement (SHELXL)*; University of Göttingen: Göttingen, Germany, 1997.